

# Applying Shower Development Universality to KASCADE Data

W.D. Apel<sup>a</sup>, A.F. Badea<sup>a,2</sup>, K. Bekk<sup>a</sup>, J. Blümer<sup>a,b</sup>, E. Boos<sup>c</sup>,  
H. Bozdog<sup>a</sup>, I.M. Brancus<sup>d</sup>, K. Daumiller<sup>a</sup>, P. Doll<sup>a</sup>,  
R. Engel<sup>a</sup>, J. Engler<sup>a</sup>, H.J. Gils<sup>a</sup>, R. Glasstetter<sup>e</sup>,  
A. Haungs<sup>a,1</sup>, D. Heck<sup>a</sup>, J.R. Hörandel<sup>b,3</sup>, K.-H. Kampert<sup>e</sup>,  
H.O. Klages<sup>a</sup>, I. Lebedev<sup>a,c,1</sup>, H.J. Mathes<sup>a</sup>, H.J. Mayer<sup>a</sup>,  
J. Milke<sup>a</sup>, J. Oehlschläger<sup>a</sup>, S. Ostapchenko<sup>a,4</sup>, M. Petcu<sup>d</sup>,  
H. Rebel<sup>a</sup>, M. Roth<sup>a</sup>, G. Schatz<sup>a</sup>, H. Schieler<sup>a</sup>, H. Ulrich<sup>a</sup>,  
J. van Buren<sup>a</sup>, A. Weindl<sup>a</sup>, J. Wochele<sup>a</sup>, J. Zabierowski<sup>f</sup>

<sup>a</sup>*Institut für Kernphysik, Forschungszentrum Karlsruhe, Germany*

<sup>b</sup>*Institut für Experimentelle Kernphysik, Universität Karlsruhe, Germany*

<sup>c</sup>*Institute of Physics and Technology, Almaty, Kazakhstan*

<sup>d</sup>*National Institute of Physics and Nuclear Engineering, Bucharest, Romania*

<sup>e</sup>*Fachbereich Physik, Universität Wuppertal, Germany*

<sup>f</sup>*Soltan Institute for Nuclear Studies, Lodz, Poland*

---

## Abstract

On basis of the theorem of a universal shower development stating that a hadronically generated extensive air shower is completely described by the primary energy, the position of the shower maximum and a parameter related to the total muon number, the so-called correlation curve method is developed and applied to KASCADE data. Correlation information of the muon and electron content of showers measured by the KASCADE experiment are used for the reconstruction of energy and mass of primary cosmic rays. Systematic uncertainties of the method and the results are discussed in detail. It is shown that by this method general tendencies in spectrum and composition indeed can be revealed, but the absolute normalization in energy and mass scale requires much more detailed simulations.

---

<sup>1</sup> corresponding authors, *E-mail address*: haungs@ik.fzk.de; lebedev@satsun.sci.kz

<sup>2</sup> on leave of absence from Nat. Inst. of Phys. and Nucl. Eng., Bucharest, Romania

<sup>3</sup> now at: Radboud University Nijmegen, The Netherlands

<sup>4</sup> on leave of absence from Moscow State University, Russia

## 1 Introduction

Due to the rapidly falling intensity with increasing energy, cosmic rays of energies above  $10^{15}$  eV can be studied only indirectly by observations of extensive air showers (EAS), which are produced by interactions of cosmic particles with nuclei of the Earth's atmosphere. The observation of a kink in the power law [1] of the size spectrum of EAS and consequently of the all-particle energy spectrum at  $\sim 3 \cdot 10^{15}$  eV has induced considerable interest and experimental activities. Nevertheless, despite of about 50 years of EAS measurements, the origin of this so-called 'knee' in the spectrum has not yet been convincingly explained [2]. In reference [3] an overview is given on current models trying to explain the origin of the knee. Many of these models predict a detailed shape of the primary cosmic ray spectrum around the knee with a specific variation of elemental composition. The experimental access to understand the knee requires accurate measurements of the energy spectra of individual cosmic ray elements.

The strategy pursued by the KASCADE collaboration invokes an unfolding procedure of the two-dimensional shower size spectrum (total electron number vs. EAS muon number) into energy spectra of five individual mass groups [4]. Despite the success of this method for the reconstruction of the shape of the spectral forms, a large uncertainty was found due to the strong dependence on the hadronic interaction models underlying the analyses. More general, any interpretation of EAS data obtained from particle detectors on ground trying to deduce the energy and composition introduces uncertainties of hadronic interactions during the shower development. On the other hand, following the theorem of the shower universality [5], each EAS can be characterized by three parameters only: the primary energy  $E_0$ , the depth of the shower maximum  $X_{\max}$ , and a parameter describing the muon component of the shower, e.g. total muon number  $N_\mu$ . It is assumed that universal functions exist depending on these three parameters parameterizing the full shower development, i.e. from these three parameters (corrected for shower-to-shower fluctuations) the elemental composition can be extracted and/or constraints can be given for hadronic interaction models. Even more, this theorem professes that the link between primary mass and energy to certain shower observables is universal, i.e. independent of a specific hadronic interaction model [6,7].

The present work is directed to investigate the possibility and accuracy of ground based EAS measurements (in case of KASCADE) of extracting elemental energy spectra of individual mass groups by assuming the simple assumptions of a universal shower development. Full Monte-Carlo shower simulations including the KASCADE detector response are used for detailed tests of the capabilities of the applied method.

## 2 Universality of the shower development

The phrase of an air shower universality states that hadronically generated showers are in many aspects similar in their development through the atmosphere. Therefore, a set of a few (e.g.  $E, X_{max}, N_{\mu}$ ) physical parameters is sufficient to investigate the composition of the primary cosmic rays and the characteristics of high-energy hadronic interactions. Previous studies have shown, that analytical or semi-empirical models for describing the shower development assume or reproduce this shower universality. For example the Heitler toy-model [8], which is based on a splitting approximation of electromagnetic cascades, relates the shower maximum and the number of charged pions to the primary energy ( $X_{max} \propto \log E_0, N_{\pi^{\pm}} \propto N_{\mu} \propto E_0^{\beta}$ ). Investigations with sophisticated Monte Carlo codes for the air shower simulation on experimentally observable parameters have demonstrated that characteristics of the electromagnetic component are universal [7,9] as well as that the universality can be used to normalize the response of a ground detector to the muon content of EAS [10].

Recently the basic idea of Heitler was invoked by Matthews [11] to reveal salient air shower characteristics, where the shower properties are related to  $E_0 = c_1(N_e + c_2 N_{\mu})$  and  $X_{max}^p = X_0 + c_3 E_0$  and  $\ln A \propto X_{max}^p - X_{max}^A$ , where  $X_0$  is the position of the first interaction,  $X_{max}^p$  the position of the shower maximum for primary protons, and  $X_{max}^A$  the shower maximum position for a particle with primary mass A, respectively. Beside the basic parameters describing the EAS the formulas contain constants  $c_i$ , the values of which are given by particle physics including interaction lengths, elongation rates and inelasticity constants. As not all of these constants are known with high accuracy from accelerator data they also express the still existing and presently unavoidable model dependence of the interpretation of air-shower data.

To obtain the three basic EAS parameters ( $E, X_{max}, N_{\mu}$ ) sophisticated air shower experiments perform hybrid measurements, i.e. measuring simultaneously the particles on ground and the longitudinal air shower development by fluorescence light detection. The energy  $E_0$  is then deduced either by the total amount of light or by the total amount of secondary particles on ground. Direct access to  $X_{max}$  is provided by fluorescence measurements; the muon number has to be obtained by ground or underground measurements.

By classical air shower experiments, i.e. arrays of surface particle detectors only, however,  $X_{max}$  is not available. For such experiments the assumptions of a universal shower development have to be introduced to reconstruct the cosmic ray composition. In most cases this is done by the use of detailed Monte Carlo simulations. However, following Matthews' argumentation, the mass A of the primary particle can be estimated less model dependent by ground

observables if the difference in  $X_{\max}$  of a certain primary mass  $A$  to  $X_{\max}^p$  is known. The assumption of shower universality is suggesting, that the EAS development is the same for all showers after the shower maximum. Hence, the difference of electron number and muon number at observation level should be a direct measure of the differences in depth of the shower maximum and consequently of the primary mass. This is the principal idea of the present studies.

In this approach we will analyze KASCADE data with the so-called correlation curve approach where ground observables are used. To reduce effects of shower-to-shower fluctuations the correlation between the measured observables are also taken into account instead of using above mentioned formulas only. For that, the original correlation curve method [12,13] was modified and as relevant parameters the correlation of the electron,  $N_e$ , and muon,  $N_\mu$ , number is considered. The modification concerns the exchange of the lateral slope of the particle distribution ('age') with the number of shower muons, as the age measured close to sea-level was found to loose most of its information on the longitudinal development. The results will be compared for different ranges in zenith angle, for different hadronic interaction models underlying the analysis, and with the results of the KASCADE unfolding procedures [4].

### 3 KASCADE experiment

The KASCADE experiment located at the site of the northern campus of the Karlsruhe Institute of Technology KIT, Germany, measures various observables of extensive air showers with primary energies between  $3 \cdot 10^{14}$  and  $1 \cdot 10^{17}$  eV. It consists of three major detector components: the field array, the muon tracking detector and the central detector complex [14]. For this analysis only the field array is of relevance, which extends over an area of  $40.000 \text{ m}^2$  and consists of 252 detector stations for detection of the electron component, where 192 stations employ in addition shielded scintillators for muon measurements. The data set used in the present analysis is similar to that one used for the unfolding analyses described in [4] and [15]. Details of the reconstruction of the shower axis direction, the total electron number and the truncated muon number (muon content in  $40 - 200 \text{ m}$  core distance, used for the present analysis) are described in [14] and [16].

### 4 Simulations

The simulations of the EAS development have been performed by using the QGSJet01 high-energy hadronic interaction model [18] in the frame of the

CORSIKA program version 6.156 [19]. For the low energy interactions ( $E_{cm} < 200$  GeV) the FLUKA [20] (version 2002.4) code, and for treating the electromagnetic part the EGS4 [21] program package was used. About 2 millions of EAS in the energy interval of  $10^{14}$  eV to  $10^{18}$  eV for each of 5 primaries (p, He, C, Si, Fe) have been simulated. The energy distribution follows a power law with slope index of -2. The zenith angles are distributed in the range  $[0 - 42^\circ]$ . In order to take into account the installation response a detailed GEANT [22] simulation of the KASCADE detectors and the reconstruction by the standard KASCADE reconstruction software was used. With less statistics the simulations were repeated with the SIBYLL (version 2.1) [23] code as high energy interaction model instead of QGSJet.

## 5 Correlation curve method and simulation studies

The sensitivity of most of EAS observables measurable at ground level to the mass of the primary cosmic ray particles is rather weak due to huge fluctuations during the shower development in the atmosphere, which can be even larger than the difference of the mean values of primary protons and iron nuclei. The main contribution to these fluctuations of  $N_e$  and  $N_\mu$  at a given observation level is connected with parameters of the first or first few interactions in the atmosphere. For example, if a 100 PeV cosmic iron comes into collision with nitrogen of the Earth's atmosphere the multiplicity of the interaction can be only a few secondary particles (peripheral or diffractive interaction) or up to hundreds of secondaries (central collision). Each of these secondary particles interact further with nuclei of the atmosphere and therefore can produce secondary shower particles in a wide interval of multiplicity. After a few generations of interactions the further development of the EAS gets more similar due to a averaging effect and the shower behaves significantly less fluctuating.

In addition, the reconstruction of EAS gets more difficult by combining different zenith angles, because EAS impinging with large zenith angles cross a thicker layer of the atmosphere and consequently vary in  $N_\mu$  and  $N_e$ . Hence, a correction of  $N_e$  and  $N_\mu$  is necessary, which leads to additional uncertainties.

A possible approach to overcome this slant depth effects can be found by correlation analyses of different observables. In this work, a correlation analysis of the number of muons,  $N_\mu$ , and electrons,  $N_e$  in the EAS is considered. By assuming the shower development universality, in contrast to the first high-energetic hadronic interactions the electromagnetic development is similar for all showers: If showers are generated with same incident parameters (energy, mass), they have a similar development - after the shower maximum. Therefore, the correlation of the electron and muon number at observation level

hints to the position of the shower maximum, i.e. in particular to the behavior of the first interactions.

### 5.1 The correlation curve method

A correlation curve is defined as a polynomial function in a two-observable plane fitted to full simulated showers of same primary characteristics.

For the energy reconstruction this methodical approach uses  $\log_{10}(N_e)$  vs.  $dN_{e\mu}$  correlation curves, where  $dN_{e\mu} = \log_{10}(N_e) - \log_{10}(N_\mu)$ . Fig. 1 (left) shows, that all showers of the same mass and energy in a wide interval of zenith angles ( $0 - 42^\circ$ ) concentrate around specific  $\log_{10}(N_e)$  vs.  $dN_{e\mu}$  correlation curves. In this presentation, the large fluctuations of  $\log_{10}(N_e)$  are reduced to smaller fluctuations around the correlation curves. By this, the use of such correlation curves allows to suppress the influence of the fluctuations (connected with parameters of the first interactions) on the energy reconstruction. A further positive aspect of this approach lies in the small dependence on the zenith angle (at least for  $< 42^\circ$ ) of the shower. Early developing EAS with small zenith angles have at observation level values of  $N_e$  and  $N_\mu$  which are close to  $N_e$  and  $N_\mu$  values of later developing showers with larger zenith angles. Hence, showers with large zenith angles help to obtain a more extended correlation curve with therefore a smaller uncertainty which leads to a more accurate determination of the primary energy. Fig. 1 (left) illustrates this by showing showers with different zenith angles.

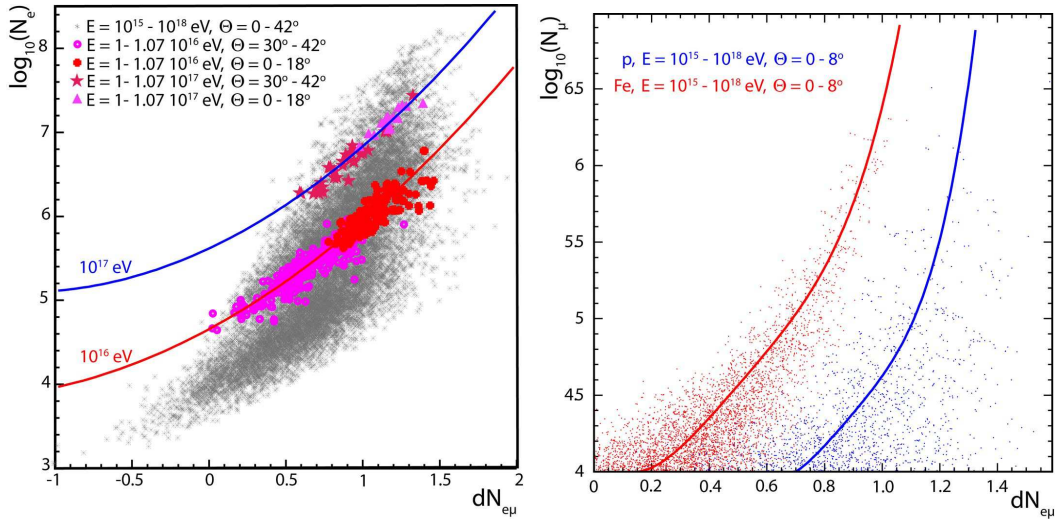


Fig. 1. Left:  $\log_{10}(N_e)$  vs.  $dN_{e\mu}$ -distribution for proton initiated EAS, simulated by QGSJet including the KASCADE detector response, and example correlation curves as used for the energy reconstruction. Right:  $\log_{10}(N_\mu)$  vs.  $dN_{e\mu}$ -dependences for iron and proton initiated showers and correlation curves as used for the mass reconstruction.

Whereas  $\log_{10}(N_e)$  vs.  $dN_{e\mu}$  correlation curves are used for energy reconstruction, for mass reconstruction  $\log_{10}(N_\mu)$  vs.  $dN_{e\mu}$  correlation curves are proposed. Most of the showers of the same mass in a wide interval of primary energy ( $10^{15} - 10^{18}$  eV, at least) are placed around such curves (see Fig. 1, right). The  $\log_{10}(N_\mu)$  vs.  $dN_{e\mu}$  correlation curves differ significantly for proton and iron showers. This allows to separate proton and iron showers (at least) with high efficiency in almost the full energy interval (at least, from  $5 \cdot 10^{15}$  to  $10^{18}$  eV). By simulations it was found that the largest source for uncertainties in the mass reconstruction at low energies ( $\log(E/\text{GeV}) < 6.5$ ) is due to uncertainties of the  $N_\mu$  reconstruction. When a shower covers a small area only and the number of hit muon detectors is small, the statistical uncertainties of  $N_\mu$  reconstruction increase and therefore the uncertainties of the mass reconstruction increase.

## 5.2 Procedure of mass and energy reconstruction

The final procedure of the energy and mass reconstruction in the present studies is realized in the following way:

- (1) For each of the simulated primaries the  $dN_{e\mu}$  vs.  $N_\mu$ -distribution in narrow bins of zenith angles is fit by a polynomial function taking  $\theta$  and  $A$  as free parameters. This yields a function  $dN(N_\mu, A, \theta)$ .

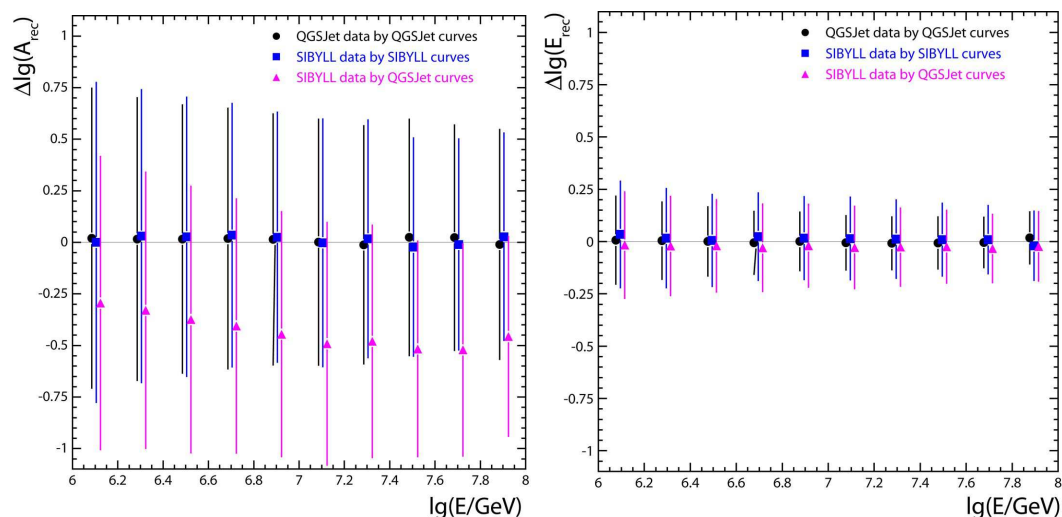


Fig. 2. Left: Accuracy in mean mass reconstruction shown for QGSJet simulations by applying correlation curves obtained by QGSJet simulations, for SIBYLL simulations by applying correlation curves obtained by SIBYLL simulations, and for SIBYLL simulations by using QGSJet for determining the correlation curves. Used are the full Monte Carlo sample of 5 primary mass groups with equal abundances. For a better visibility some markers are displaced. Right: Accuracy in energy reconstruction. Same notation as in left figure.

- (2) The mass of the showers is determined from the function by varying  $A$  and minimizing the difference between the measured  $dN_{e\mu}$  and the function  $dN(N_\mu, A, \theta)$  at fixed (measured)  $\theta$  and  $N_\mu$ .
- (3) Using simulations for different fixed energies and masses the  $\log_{10}(N_e)$  vs.  $dN_{e\mu}$  - distributions are fit with a polynomial function taking  $E_0$  and  $A$  as free parameters. This yields a function  $\log_{10}(N_e(dN_{e\mu}, E_0, A))$ .
- (4) The primary energy is determined from this function by varying  $E_0$  and minimizing the difference between the measured  $\log_{10}(N_e)$  and the function  $\log_{10}(N_e(dN_{e\mu}, E_0, A))$  at the fixed (measured)  $dN_{e\mu}$  and fixed (reconstructed)  $A$ .

Figure 2 shows the obtained accuracies for the mass and energy reconstruction by this procedure. While the energy reconstruction shows only a small dependence on the interaction model and a smaller width of the distribution, the dependence on the models and the width is larger in case of the mass reconstruction. In particular, if one fits the correlation curves based on one model and applies these curves to a test data set generated by the other model, a clear systematic shift is observed. Inside one model the reconstruction is accurate, meaning the shower universality is preserved, even after detailed simulations including the full chain of Monte Carlo shower simulation, detector simulation, and the reconstruction. This behavior is not surprising as the constants in, for example, Matthews's interpretation of Heitler's approximation depend on the model of the hadronic interactions. In addition, this is the basis of differences between QGSJet and SIBYLL.

In the simulation program CORSIKA different hadronic interaction models are used for high energy ( $E_{lab} > 200 \text{ GeV}$ ) and low energy ( $E_{lab} \leq 200 \text{ GeV}$ ) interactions. Hence, the high energy models control especially the first few interactions of an air shower, whereas most of the (electromagnetic) particles detected at ground level are generated by the low energy interaction models. Two important parameters characterizing the high-energy interaction models are the inelastic cross section and the elasticity of the interaction. A lower cross section implies a longer mean free path for the hadrons in the atmosphere and thus a reduction of number of interactions. Showers develop more slowly and the mean  $N_\mu/N_e$  ratio at ground level decreases. A lower elasticity implies that less energy is transferred to the leading particle. It enhances the possibility to produce secondary particles as more energy is available for multi-particle production. Showers develop more quickly and the mean  $N_\mu/N_e$  ratio at ground level increases.

SIBYLL has a larger (compared to QGSJet) inelastic cross section and a larger elasticity. This means that we are faced with two competing processes influencing the number of particles observed and the position of the shower maximum. Whereas, the depth of the shower maximum, predicted by SIBYLL and QGSJet are close to each other, SIBYLL 2.1 simulations predict about



8% smaller muon number and 10-20% larger electron number than QGSJet 01 [26]. These differences in the predictions of muon and electron numbers at the observation level lead to the significant effect for the mass reconstruction. Consequently, investigations with further high-energy hadronic interaction models (e.g. the newly developed EPOS model [28]), with again different predictions on the electron-muon number ratio, would lead to varying mass reconstruction and therefore varying results in the interpretation of measured data in means of composition. The influence of using different low energy interaction models (FLUKA and GHEISHA) was found to be negligible for the discussed observables [15].

### 5.3 Energy spectra of individual mass groups

A crucial element in reconstructing energy spectra of individual masses (mass groups) is the intrinsic mass resolution of the used observables and of the method applied. Whereas the energy reconstruction is based mainly on the total number of particles, the mass reconstruction is based on the correlation of the electron and muon component leading to much larger uncertainties. Figure 3 depicts the mass resolution in case of QGSJet and shows, that with the simple ansatz used, the medium masses are not satisfactorily resolved. We remark here, that this feature was the reason to go a step forward to a more sophisticated investigation of the event-by-event correlations, resulting in the analysis described in [4]. But it is also seen, that by all means, a separation in two mass groups light and heavy is possible. Hence in the further application, we divide the data set in two parts: in a sample of light induced showers ('L') with a reconstructed mass of  $A < 12$ , and a sample of heavy induced showers ('H') with  $A \geq 12$ , respectively. This mass cut is chosen in a way that the CNO group is separated to  $\approx 50\%$  in the light and the heavy group, respectively.

Before we apply the correlation curve method to the measured data, the reconstruction procedure is tested with an artificial test sample. For that we use as input in gross features the unfolding result of [4] (based on QGSJet), i.e. the spectra and relative abundances of five primary mass groups, for the present studies grouped in ratios of light and heavy primaries, respectively, to the total amount of events. This input composition is displayed in Fig. 4 with index *gen*. The application of the reconstruction steps to this test sample results in the reconstructed relative numbers of heavy and light as displayed in Figure 4 (index *rec*). For obtaining a reliable result still missing is the deconvolution of systematic uncertainties in mass reconstruction and energy estimation leading to a correction of the reconstructed individual mass spectra. The mis-classification probabilities are obtained from simulations with the assumption of equal number of primaries in four generated mass groups. As a first step a test sample is considered with equal abundances of Fe and

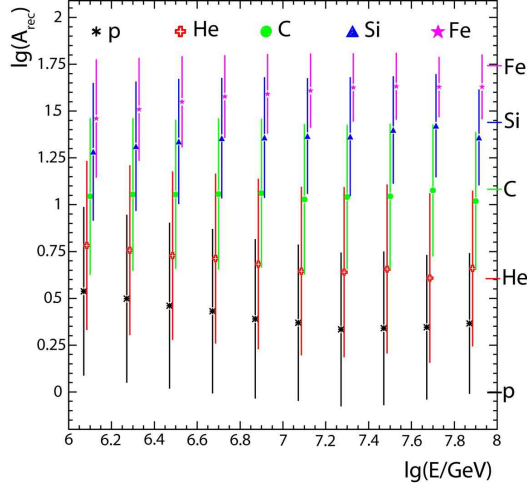


Fig. 3. Resolution in mass reconstruction (QGSJet based). Equally weighted number of primaries are generated and the resulting mean mass  $\lg(A)$  and the width of the distributions are shown in dependence of the primary energy.

Si forming the heavy group and equal abundances of p and He forming the light group. In order to check the accuracy of the method, we repeated these tests comparing output data with different input compositions and by that we calculated the maximal possible uncertainty due to the composition within the individual mass groups.

Thus, the final results are the spectra corrected for the energy-dependent misclassification probabilities (index *cor*). The upper and lower lines in Fig. 4 limit the maximal uncertainty of this correction due to the unknown, but assumed composition inside the light and heavy groups (ratio of protons to Helium and Si to Fe, respectively for the calculation of the misclassification probabilities). Where in the left part of the figure everything is based on the QGSJet model, for the right part the result is shown if the input spectra are generated with QGSJet and the whole reconstruction is based on values obtained by using the SIBYLL model. These investigations show that the shape of the distribution is preserved but SIBYLL reconstructs a heavier composition. Comparing the test results for QGSJet and SIBYLL, it is obvious that the largest difference is due to the hadronic interaction model.

In summary, the correlation curve method is able to confirm the shower universality in basic considerations. This finding is due to the fact, that by investigating the total number of secondary particles together with the difference in electron and muon number at ground level it is possible to reconstruct the primary energy and to classify in two mass groups, at least. In addition, the method avoids to a large amount the problem of correction of  $N_e$  and  $N_\mu$  for EAS with different zenith angles (and uncertainties connected with the correction). The largest deficiency of the described reconstruction procedure is due to the large shower-to-shower fluctuations, anyhow not considered in the

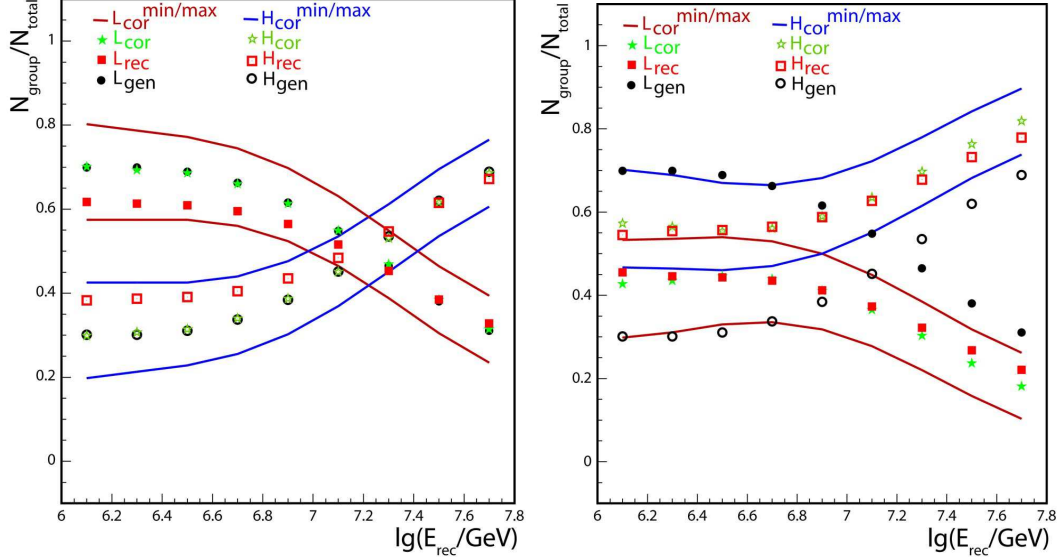


Fig. 4. Comparison of simulated (index *gen*) and reconstructed elemental mass spectra (light and heavy in terms of relative abundances) before (index *rec*) and after (index *cor*) correction for the mis-classification. The lines limits the maximal possible uncertainty due to the composition within the mass groups. Statistical uncertainties are not shown. Left: QGSJet based (generation and reconstruction). Right: SIBYLL based reconstruction, but QGSJet based generation of the test sample.

assumptions of simple Heitler-based models.

## 6 Application to KASCADE data

The correlation curve method as described in the last chapter is applied to the KASCADE data set, where a ‘good-run’-selection of KASCADE is used. In these runs all clusters and all detectors are present and working and are well calibrated. In total the used sample sums up to about 993 days measuring time. This is the same sample as used in ref. [4], the KASCADE unfolding analysis of the two-dimensional shower size spectrum.

In Figure 5 the reconstructed all-particle spectrum is shown together with the spectra of light and heavy induced showers for the zenith angular range of  $0 - 18^\circ$ . The left panel of the figure shows the result by using QGSJet based simulations, the right panel for the SIBYLL model. The horizontal error bars denote the uncertainty in energy reconstruction. The vertical error bars combine the statistical uncertainty of both, data and simulations with the uncertainty due to the misclassification probabilities. The lower and upper limits shown in the plots describe the maximum uncertainty due to the assumption of a composition in the calculation of the mis-classification probabilities.

Knee like features are clearly visible in the all-particle spectrum of both results, QGSJet and SIBYLL based, as well as in the spectra of light primaries. This demonstrates that the elemental composition of cosmic rays is dominated by light components below the knee and dominated by a more heavy component above the knee feature. Thus, the knee feature originates from a decreasing flux of the light primary particles. This observation corroborates results of the analysis of the unfolding procedures described in [4] and of muon density measurements at KASCADE [24], which were performed independently of this analysis, as well as results from the EAS-TOP [25] experiment.

Comparing QGSJet based with SIBYLL based results, the all particle spectrum as well as the characteristics of the individual mass group spectra (dis-

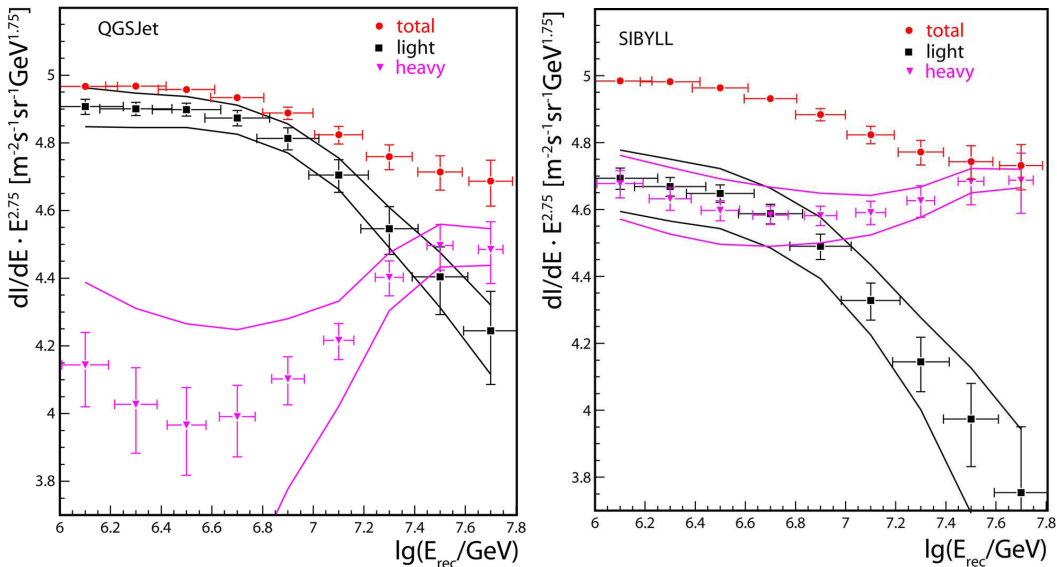


Fig. 5. KASCADE energy spectra reconstructed for the zenith angular interval of  $\theta = 0 - 18^\circ$ , calculated by applying the correlation curve method on the basis of the QGSJet-FLUKA model (left) and based on the SIBYLL-FLUKA (right) model. For the description of the error bars see text.

tinct knee feature for the light components, but not for the heavy ones) are in remarkable agreement, but there are large differences in the relative abundances of the different primaries. This confirms that the assumption of a universal shower development is valid, in particular for the evolution of the shower in the atmosphere. This is not true for the absolute number of particles on ground, where large differences in the model predictions occur. It is obvious that the obtained individual energy spectra (especially for the relative abundances of the different mass groups) depend also on the reconstruction method and/or the low energy interaction model, but the main differences stem from varying the high-energy hadronic interaction model.

To deepen the understanding and as cross-check of the source of the differences in the two results, the correlation curve method is applied to data in different

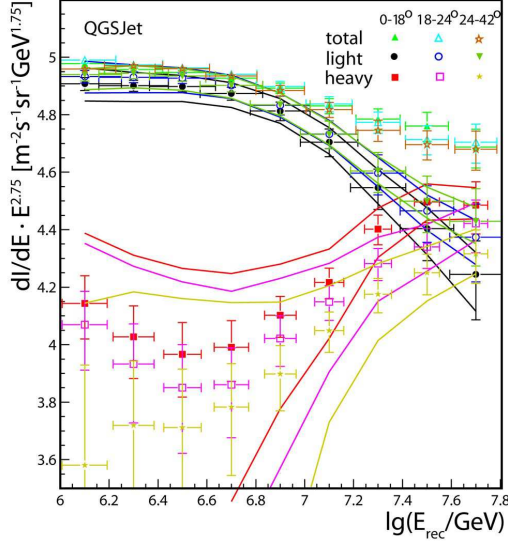


Fig. 6. Comparisons of the QGSJet based results for different angular ranges.

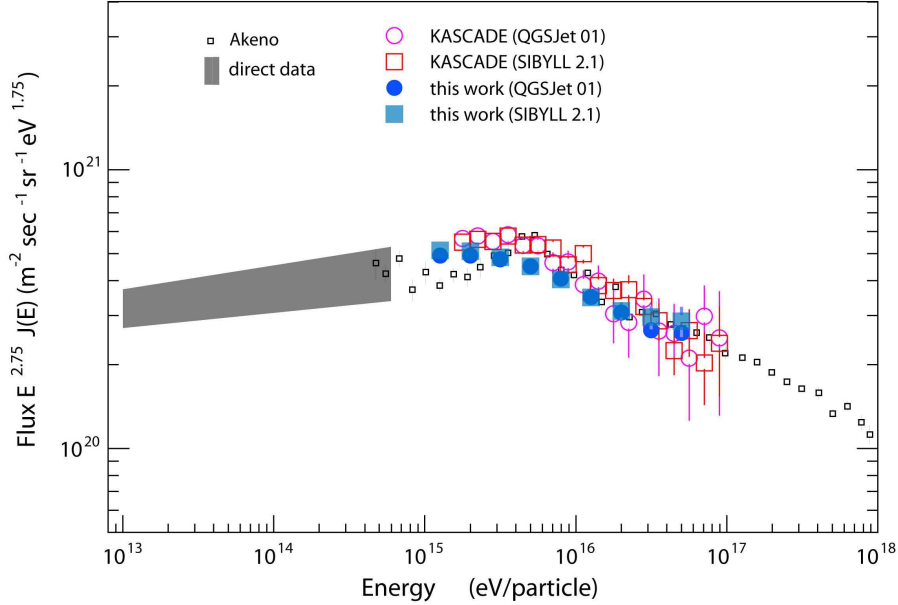


Fig. 7. The all-particle spectra obtained on basis of two different hadronic interaction models. Only statistical error bars are shown. Results of the KASCADE unfolding analysis [4] and the AKENO experiment [29] are also shown, as well as a compilation of direct measurements [27].

zenith angular bins. Fig. 6 displays the resulting energy spectra for different ranges in zenith angle (in case of QGSJet). The all-particle spectrum as well as the relative abundances of the different mass groups are in good agreement, confirming differences in the different hadronic interaction models as main source of diverging results.

Finally, in Figure 7 the resulting all-particle spectra are compared with the results based on the unfolding procedure [4] with the same high energy inter-

action models and on the same data set ( $0 - 18^\circ$ ). Differences are due to the reconstruction method and the use of a different low energy interaction model (FLUKA here instead of GHEISHA), where the influence on the low energy interaction model was found to be of minor importance [15]. In addition, a compilation of direct measurements [27] and the results from the AKENO [29] experiment are included as well. The present result on the all-particle spectrum is essentially independent of the interaction model used and in good agreement with results from other experiments.

## 7 Discussion and conclusions

Based on the assumption of a universality of the shower development in air, observables were extracted measurable by a ground based particle air shower experiment. The theorem of shower development universality asserts that the shower can be fully described if the energy, the position of the shower maximum and a normalized characteristics of the muon content of the shower are known. In particular, by having these values, the primary mass and the mechanisms of the first or few first highest energy interactions can be inferred.

In this work, investigating KASCADE data and therefore relying on ground observables, only, we defined the logarithmic difference of ground measured electron and muon numbers as the parameter connected with the position of the shower maximum. This connection is grounded on studies of Matthews [11] revealing salient air shower characteristics by simple formulas based on the assumptions of a universal shower development. As method of reconstructing the primary mass and energy of the showers the correlation curve method is applied taking into account not only the total electron and muon number of the shower, but also the correlations between the used observables. In addition, using invariant correlation curves of reconstructed  $N_e$  and  $N_\mu$  allows significantly to decrease the influence of shower-to-shower fluctuations on the reconstruction of energy and mass of the primary cosmic rays. Uncertainties of the energy reconstruction are almost independent of the slope of initial energy spectrum and initial mass composition. Furthermore, in this approach the energy reconstruction is nearly independent of the zenith angle (at least for  $\Theta < 42^\circ$ ).

By detailed simulation studies the energy and mass reconstruction accuracies could be estimated, demonstrating that indeed the connection between the ratio of electron to muon number to the position of the shower maximum is given, and therefore a sensitivity to the primary mass is maintained in the ground observables. I.e., a universality in the shower development is grossly given. This concerns in particular the ratio of muons to electrons, but is less valid for the absolute numbers of particles on ground and neglects the effect

on shower-to-shower fluctuations. The description of an universal behavior of the shower development is given probably for all the widely used simulation codes and interaction models, even if in the present studies this was tested in detail only for the models QGSJet and SIBYLL.

Therefore, to quantify the energy spectrum and mass composition, hadronic interaction models still are needed. In particular, the normalization to the absolute value of the energy and to the mass have to make use of models. In terms of the revised Heitler model [11] it means, that the constants in the given formulas have to be defined, which need input from particle physics. The relative behavior of the measured showers (shape of the spectrum and composition changes), however, can be revealed by assuming basic shower development considerations, i.e. applying the shower universality. However, shower-to-shower fluctuations are annoying for a simple application of the universality theorem. Especially, following the shower to sea-level, the assumptions are too simple and underestimate the fluctuations (which is possibly also true for full Monte Carlo simulations).

By applying the correlation curve method to fully simulated KASCADE EAS, it was found that a proper mass discrimination is possible only in two mass groups - light and heavy induced showers. Again the largest uncertainty is in mass estimation and by choosing different hadronic interaction models, in this case by comparing QGSJet and SIBYLL. As guessed by the universality theorem, energy spectra and shape of the relative composition are revealed to be quite stable, but the absolute normalization to the mass scale is different leading to a much larger (heavier) mean mass in case of SIBYLL. Modified or newly developed hadronic interaction models with changes of the interaction mechanisms probably would take us to other, changed abundances.

Finally the reconstruction procedure was applied to KASCADE data, resulting in QGSJet and SIBYLL based all-particle spectra as well as energy spectra of the light and heavy groups. The results are in good agreement with other experiments, in particular with results of the much more sophisticated ansatz of unfolding the two dimensional size spectrum measured by KASCADE.

As basic conclusion by this investigation we can confirm that the composition gets heavier and heavier crossing the knee in the all-particle spectrum due to the fact that the showers become muon-richer. This was found in many experiments by using detailed simulations [4] or simple models or assumptions on the universal shower development [24], only. The present study could show that very strong changes in the description of hadronic interactions have to occur and completely overruling the shower development universality if one would explain the knee without changing composition. As an example in this direction, in [30] the effect of percolation, i.e. an increase of the energy part into one leading pion, is discussed. The mechanism would change the inelasticity

of the interactions, and therefore the basic correlations of shower observables. But the effect, if true, can be expected for energies above 100 PeV, only and is anyhow not strong enough to explain the very distinct knee feature.

In summary, assuming the shower development universality to be true in its basic features it is clear, that there is a knee in the all-particle spectrum at a few PeV, and that this knee is due to a kink in the spectrum of light primary particles.

## Acknowledgements

This work is supported by the Deutsche Forschungsgemeinschaft (DFG grants GZ436KAS17/1/04 and 436KAS17/1/07) and by the Kasach Academy of Science, what is gratefully acknowledged by I.L. and A.H..

## References

- [1] Kulikov G.V., Khristiansen, Soviet Physics JETP 35 (1959) 441.
- [2] Haungs A., Rebel H., Roth M., *Rep. Prog. Phys.* **66** (2003) 1145.
- [3] Hörandel J.R., *Astropart. Phys.* **21** (2004) 241.
- [4] Antoni T. et al. - KASCADE-Collaboration, *Astropart. Phys.* **24** (2005) 1.
- [5] Chou A.S. et al., 2005, Proc.29<sup>th</sup> ICRC, Pune, **7** (2005) 319.
- [6] Giller M. et al., 2004, *J. Phys. G: Nucl. Part. Phys.* **30** 97.
- [7] Nerling F. et al., *Astropart. Phys.* **24** (2006) 421.
- [8] Heitler W., *Quantum Theory of Radiation* Oxford University Press (1944).
- [9] Gora D. et al., *Astropart. Phys.* **24** (2006) 484.
- [10] Schmidt F. et al., 2007, Proc.30<sup>th</sup> ICRC, Merida (2007), in press.
- [11] Matthews J., *Astropart. Phys.* **22** (2005) 387.
- [12] Boos E.G. et al., 2001, Proc.27<sup>th</sup> ICRC, Hamburg, p.269
- [13] Boos E.G. et al., *Kaz.J. Izv.AS RK ser.fiz.-mat.* **N 2** (2002) 68.
- [14] Antoni T. et al. - KASCADE-Collaboration, *Nucl. Inst. Meth. Phys. Res. A* **513** (2003) 490.
- [15] Ulrich H. et al. - KASCADE-Grande-Collaboration, *Nucl. Phys. B (Proc. Suppl.)* (2007), in press.



- [16] Antoni T. et al. - KASCADE-Collaboration, *Astropart. Phys.* **14** (2001) 245.
- [17] Haungs A. et al. - KASCADE-Grande collaboration, 2003, Proc.28<sup>th</sup> ICRC, Tsukuba, HE1.5, p.985
- [18] Kalmykov N.N., Ostapchenko S.S., *Sov.J.Yad.Fiz.* **56** (1993) 105.
- [19] Heck D. et al., FZKA-Report 6019, Forschungszentrum Karlsruhe, 1998
- [20] A. Fasso et al., Proc. Monte Carlo 2000 Conf., Lisbon, Oct. 23-26, 2000, A. Kling et al. eds., Springer (Berlin) 955 (2001).
- [21] Nelson W.R., Hirayama H. and Rogers D.W.O., *Report SLAC 265*, Stanford Linear Accelerator Center (1985).
- [22] CERN, *GEANT - Detector Description and Simulation Tool*, CERN Program Library Long Writeup **W5013**, CERN (1993).
- [23] Engel R. et al., *Proc. 26<sup>th</sup> Int. Cosmic Ray Conf.* Salt Lake City (USA) **1** (1999) 415;  
Engel, J. et al., *Phys. Rev. D* **46** (1992) 5013.
- [24] Antoni T. et al. - KASCADE-Collaboration, *Astropart. Phys.* **16** (2002) 373.
- [25] Aglietta T. et al. - EAS-TOP-Collaboration, *Astropart. Phys.* **21** (2004) 583.
- [26] Milke J. et al. - KASCADE-Collaboration, *Proc. 27<sup>th</sup> Int. Cosmic Ray Conf.* Hamburg **1** (2001) 241.
- [27] Watson A.A., Proc. 25th Int. Cosmic Ray Conf. (Durban) Invited, Rapporteur, and Highlight papers, p 257 (1997).
- [28] Werner K., Liu F.M. and Pierog T., *Phys. Rev. C* **74** (2006) 044902.
- [29] M. Nagano et al., *J. Phys. G: Nucl. Part. Phys.* **10** (1984) 1295.
- [30] Alvarez-Muniz J. et al., *Astropart. Phys.* **27** (2007) 271.